Research Into Payload Swaying Reduction Through Cable Length Manipulation During Boom Crane Motion

Alexander A. Kostikov
Associate Professor
Informatics and Engineering Graphics Department,
Faculty of Machine Automation and Information Technology,
Donbass State Engineering Academy,
Ukraine

Alexander V. Perig
Associate Professor
Manufacturing Processes and Automation Engineering Department,
Faculty of Machine Automation and Information Technology,
Donbass State Engineering Academy,
Ukraine

Oleksii V. Larichkin
Ph.D. Applicant (Ph.D. Candidate)
Manufacturing Processes and Automation Engineering Department,
Faculty of Machine Automation and Information Technology,
Donbass State Engineering Academy,
Ukraine

Alexander N. Stadnik
Senior Lecturer
Department of Technical Mechanics,
Faculty of Machine Automation and Information Technology,
Donbass State Engineering Academy,
Ukraine

Eduard P. Gribkov
Associate Professor
Automated Metal Forming Process and Machinery Department,
Faculty of Mechanical Engineering,
Donbass State Engineering Academy,
Ukraine

This paper is focused on an investigation into the control dynamics of a boom crane through a study of guided payload pendulum motion with a non-uniformly rotating boom-driven pivot center and variable cable length. A time-optimal control problem was formulated and numerically solved with constraints on the allowable payload swaying value using JModelica.org freeware with Optimica extension. Solutions of the optimum speed problem for the dynamic model describing the movement of the payload from the initial position to the final position are found, taking into account the nonlinearities associated with the Coriolis force, and the change in cable length during the motion. Two cases are considered: with and without taking into account the constricts on the swaying value. It was found that taking into account the constricts on the swaying value leads to an overshoot of the phase variable length. The obtained results can be used for cargo transportation by crane in various fields: industry, construction, etc. The resulting control will allow a reduction in cargo transfer time, which will lead to an increase in labor productivity. It will also reduce the amount of payload swaying, which will reduce the likelihood of injury during loading and unloading operations. The model is nonlinear, and the Coriolis force and other nonlinearities are taken into account. The model is electromechanical; the characteristics of the electric motors of the tower and the winch are taken into account. A comparative analysis of the problem of optimal control with and without allowance for restrictions on the cargo swaying value is provided and differences in the control functions for each of these cases are defined. The optimal control, taking into account the change in rope length, allows the solution of practical tasks in moving the cargo, taking into account the presence of obstacles that arise on the way of the cargo.

Keywords: *Boom crane, cable length variation, payload swaying, absolute trajectory, electric drive control, optimal control problem, JModelica.org freeware, numerical simulation.*

1. INTRODUCTION

1.1 The state of the art and review

The development trends of modern controlled crane dynamics include: complication of mathematical models of the system by increasing the number of degrees of freedom (DoFs), application of more sophisticated control methods, accounting for external nondeterministic disturbances such as a constant or random wind load [1-22].

At the present stage of the development of research instruments, a general approach to the analysis of controlled crane dynamic systems should consider the electromechanical system as a complex of interrelated subsystems. In this case, subsystem 1 is a representation of the unchangeable part of the original crane system in the form of a complex of ordinary differential equations (ODEs) and/or differential algebraic equations (DAEs) with constant coefficients determined by the parameters of the system. Subsystem 2 is a control subsystem in which servo communications, open and closed loop control algorithms of the original system, and digital and analogue state variable regulators are used. Subsystem 3 consists of modern control approaches. Accounting for the elasticity of the crane construction leads to the complication of the differential equations of the controlled crane system too. Along with classical approaches to the synthesis of correcting devices, new modern approaches have also been widely used.

The choice of a particular or specific technique is completely determined by the goal that needs to be achieved: increasing of the speed of manipulation operations, increasing the accuracy of positioning the

Received: October 2018, Accepted: February 2019
Correspondence to: Dr Alexander V. Perig
Donbass State Engineering Academy, Akademichna (Shkadinova) Str 72, 84313, Kramatorsk, Ukraine
E-mail: olexander.perig@gmail.com
doi: 10.5937/fmet1903464K

load at the boundary points of the trajectory or throughout the entire process of load transportation, or increasing energy savings during the operating cycle of the crane system etc. [1-22].

According to the Abe's (2013) article [1], the length of the pendulum cable was controlled to reduce swinging of the payload in the 2D case, shown in Fig. 1 of Abe's research [1]. A feedback control, that contains terms proportional to the change in the cable length, its speed, and the cable angle of deviation from the vertical, was used in Abe's approach [1]. So, the task of constructing the automatic control law was reduced to finding three coefficients, which are optimization parameters and determine the feedback gain factors [1]. To optimize these coefficients, a numerical Particle Swarm Optimization (PSO) technique was used [1].

Abdel-Rahman and Nayfeh (2002) have proposed both 2D and 3D mechanical models of boom crane-assisted lifting and pulling down of cargo [2]. Abdel-Rahman and Nayfeh (2002) have developed their 2D model by making the assumption that the angular acceleration of the crane boom tip can be described by harmonic law [2]. The equation for small motion of the crane boom tip in the vicinity of the equilibrium position was derived by accounting for the first two terms of the Taylor series expansion of the payload's forced motion equation [2]. This linearized boom tip slow motion equation was analytically solved by a multiple scales computational technique [2]. They found that using a 2D model yields numerical simulation results with delay and lag [2]. They also showed that it is more efficient and preferable to solve this class of problems using 3D models only [2]. Abdel-Rahman and Nayfeh (2002) have derived their 3D model through the use of Lagrange equations of the second kind [2]. They have reduced the quantity of governing equations for boom-assisted payload motion from three to two in their 3D model by eliminating the geometric constraint equation for the cable length [2]. The amplitude and phase of the oscillatory motion of the crane boom tip were determined with a multiple scales analytical technique with their 3D model [2]. The stationary analytical solution as well as conditions for stability of this solution were determined for their 3D model [2]. Gain-frequency characteristics for the nonlinear 3D model were derived and plotted in [2]. In this paper Abdel-Rahman and Nayfeh have estimated the influence of both cable length and payload lifting rate on payload swaying [2]. They also found that it is possible to achieve suppression of payload swaying by changing cable length in both the upward and downward direction.

Sato and Sakawa (1988) have developed an original approach to formulation and solution of the electromechanical optimization problem of payload swaying reduction [17]. Sato and Sakawa (1988) have developed a dynamic model of flexible rotary crane control with three degrees of freedom (crane rotation, load lifting, boom lifting) [17]. The goal of the optimal control was load delivery to the desired position in such a way that at the end of the transfer the swaying of the load would decrease as quickly as possible [17]. They have implemented a stage-by-stage approach to the control process for the studied dynamic system [17]. For this goal, two types of control have been applied [17]. Initially, the control loop is open in order to ensure the transition of the dynamic system to the stability threshold (to bring the system to the equilibrium boundary) [17]. Open-loop control has been used for load movement to the desired position [17]. Then, after delivery of the payload to the desired position, the feedback coupling is turned on in the system to minimize the time required for the complete decay of the residual payload oscillations [17]. Feedback control has been applied for oscillation damping at the end of the transfer [17]. Another distinctive feature of the study [17] is the additional mechanical accounting for a new degree of freedom associated with the linkage joint in the two-component rotary crane boom structure [17]. Generality of the created model, which takes into account load lifting, boom rotation, and boom lifting should be attributed to the dignity of the model [17]. Also, the original constructed optimal control strategy should be noted, which allows switching from open-loop control to feedback control [17]. However, the important phase variables like the angle between the cable and the vertical as well as the additional angle introduced by the linkage joint between the two parts of crane boom, were linearized and simply approximated as negligible infinitesimal quantities [17]. This approximation and linearization of phase variables resulted in the fact that the derived optimal control solution of this problem was valid only for small oscillations of the dynamic system [17]. The disadvantage of such control is the possibility of significant swaying during the transfer of the load from one position to another, which is unsafe [17]. Also, the absence of experiment should be noted, and therefore the impossibility of a comparison of the modeling results and empirical data [17]. Technical implementation of the proposed optimal control is lacking also [17].

In Sawodny et al.'s (2009) paper [18] in fig. 8 and fig. 11 the experimental absolute trajectories of payload swinging are shown. These were derived for the case of slewing motion of the full-scale model of the Liebherr Harbor Mobile Crane [18]. However, the computational scheme in fig. 5 of Sawodny et al.'s (2009) paper [18] assumes the appearance of payload oscillations only in the vertical plane. This simplifying assumption does not allow Sawodny et al.'s research [18] to properly address and account for the Coriolis inertial forces. Therefore, experimental absolute paths of payload motion in figs. 8, 11 of Sawodny et al.'s (2009) paper [18] cannot be properly theoretically modeled with the extra-simplified Sawodny et al.'s model, shown in fig. 5 of [18].

Uchiyama et al (2013) have proposed suppressing the residual sway of the load of the rotary crane only due to the horizontal movement of the boom [22]. From their point of view, such an approach, i.e. leveling the possibility of suppressing the residual swaying of the load, also due to the vertical movement of the boom, will make the crane system safer and more economically preferable during its operation [22]. The peculiarity of their study was the exclusion of the need for a direct measurement of the load swing, which also reduces the total cost of the sensors entering the system

[22]. The rationale for this approach was the use of a simple velocity trajectory template widely used today (S-curve) [22]. A drawback of the work [22] is the number of assumptions made when simplifying the original differential equations of the dynamic crane system. The initial system has undergone linearization, and when recording the original equations only the most significant forces have been taken into account: centrifugal force and Coriolis force [22]. At the stages of modeling and experiment, the length of the cable, with fixed load at the end, was assumed constant [22]. Consequently, the possibility of using length variation of the cable outlet for suppressing the residual load swaying was not considered [22]. However, it should be noted that the modeling and experimentation results turned out to be very similar, which implies that the approach proposed by the authors is really workable [22].

1.2 Aims and scopes of the present research

The goal of the study is the reduction of the load swing during controlled boom rotation with a simultaneous controlled change of cable length.

The object of the study is the development of a dynamic mode of controlled load movement via the electromechanical system "electric drive – boom – load", considering variable cable length.

The subject of the study is optimal control of electric drives, providing controlled movement of the load, which minimizes the time of load movement during boom rotation and determines the allowable swinging in case of variable cable length.

A mathematical model has been developed which takes into account the nonlinearities associated with the Coriolis inertia force and the unevenness of angular portable rotation.

In the electromechanical part of the system, control processes have been applied during the acceleration and deceleration of the electric motor by introducing the term responsible for the damping.

For the constructed model of the dynamic system, the optimal control problem has been posed and numerically solved, minimizing the time of load transfer with restrictions on the amount of load swing.

A numerical analysis of simulation results has been performed with and without accounting for restrictions on swinging. The interpretation of the results is given.

For an open-loop system there is no need for calculation and technical implementation of regulators. The solution of the optimal control problem is to find the time dependences of the anchor voltage separately for each electric drive (tower, winch).

1.3 Prime novelty statement of research (highlights)

In most of the previous articles, nonlinearities have not been taken into account. Instead, linearization has been used.

In this paper, the problem of optimal control has been solved taking the nonlinearities into account, which is very important in the case of open-loop control.

The open-loop control problem has been solved numerically, taking the nonlinearities into account.

The problem of optimal performance has been solved with and without accounting for the restrictions on the amount of swing.

A comparative analysis of the above results has been given.

The developed optimal control can be implemented in software and hardware.

Controls sufficient for the hardware implementation have been found.

Taking into account the variability of length allows us to find the optimal control that provides maximum performance compared with other controls, which is especially important for the periods of acceleration and deceleration.

The efficiency of the cable length changing during the stages of acceleration and deceleration has been shown.

The contribution to the field of crane dynamics is the original dynamic system for which a new optimal performance problem has been formulated and solved.

The solution of a practical task of avoiding obstacles during load transportation by the boom crane can be realized by changing the cable length.

2. COMPUTATIONAL APPROACH

2.1 Mechanical formulation of the problem and governing equations

A three-dimensional model of a boom crane is shown in Figure 1. This is a model of a three-dimensional dynamic system that consists of:

a boom (DB),

a cable ($BM(t)$), the length of which ($l(t)[m]$) can be varied with a winch,

the torque of which depends on the voltage ($U_1(t)[V]$) applied to the anchor circuit of the electric winch motor, and

the swinging payload (M), suspended on the cable $BM(t)$).

The movement of this dynamic system is shown in Figure 1. The system has 4 (four) degrees of freedom:

the angle of rotation of the crane boom ($\varphi_e(t)[rad]$);

the angle of winch rotation ($\theta(t)[rad]$), which determines the current length of the cable ($l(t)[m]$); and

2 (two) relative angular coordinates ($\alpha_1(t)[rad]$) and ($\alpha_2(t)[rad]$).

The absolute motion of payload (M) in Figure 1 is combined (compound) motion, which includes both relative and translational (transportation) motions of point material particle (M).

The relative motion of load (M) is a spherical motion of particle (M) about a point (B), which has 3 (three) degrees of freedom and is determined by spherical angles ($\alpha_1(t)[rad]$), ($\alpha_2(t)[rad]$), and ($\theta(t)[rad]$). The first spherical angle ($\alpha_1(t)[rad]$) is the angle of deflection of cable ($BM(t)$ from the vertical (O_1z_1). The second spherical angle ($\alpha_2(t)[rad]$) determines the precessional motion of particle (M). The second angle ($\alpha_2(t)[rad]$) is the dihedral angle between the two vertical planes ($x_1O_1z_1$) and (BMO_1M_1). The first vertical plane ($x_1O_1z_1$) is perpendicular to the crane boom (DB). The second

vertical plane (BMO_1M_1) passes through the line segments (BM), (BO_1), (MM_1) and (O_1M_1). Both spherical angles ($\alpha_1(t)[rad]$) and ($\alpha_2(t)[rad]$) determine the nutational character of the relative motion of payload (M).

The rotational motion ($\varphi_e(t)[rad]$) of the tower (O_2D) with crane boom (DB) determines the translational motion of payload (M).

The absolute motion of payload (M) in Figure 1 is the resulting motion, which is the vector sum of relative and translational motions of point material particle (M).

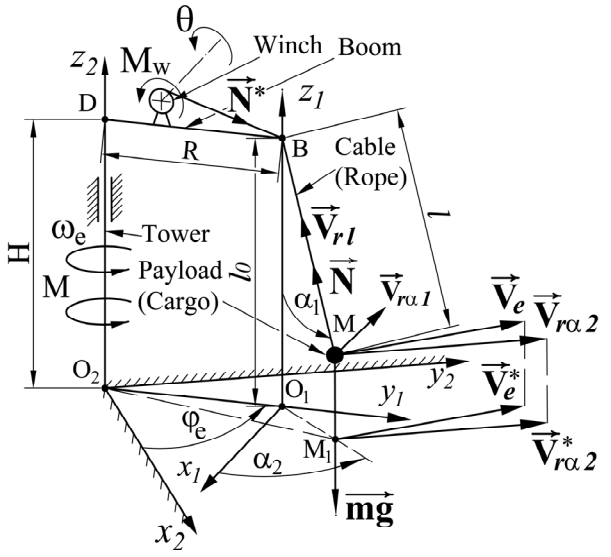

Figure 1. Three-dimensional model of the boom crane

The control of this dynamic system is carried out by 2 electric motors:

the tower motor, the output torque of which ($M(t)$ [$N{\cdot}m$]) depends on the applied control voltage ($U_2(t)$ [V]),

and the winch motor, the output torque ($M_w(t)[N{\cdot}m]$) of which depends on the applied control voltage ($U_1(t)$ [V]).

The following velocity vector components [m/s] are shown in Figure 1:

($V_{rl}(t) = (d(l(t))/dt)[m/s]$) and vector $\left(\vec{\mathbf{V}}_{rl}(t)\right)$ is directed along cable ($BM(t)$);

vectors $\left(\vec{\mathbf{V}}_{r\alpha_1}(t)[m/s]\right)$ and $\left(\vec{\mathbf{V}}_{r\alpha_2}(t)[m/s]\right)$ are perpendicular to the cable $BM(t)$);

vector $\left(\vec{\mathbf{V}}_{r\alpha_1}(t)[m/s]\right)$ is in the vertical plane (BMO_1M_1);

$$\left(\left|\vec{\mathbf{V}}_{r\alpha_1}(t)\right| = V_{r\alpha_1}(t) = \left(\dot{\alpha}_1(t)\right)\cdot l(t) = \left(\dot{\alpha}_1(t)\right)\cdot\left(BM(t)\right)\right)$$

[m/s]; where vector $\left(\vec{\mathbf{V}}_{r\alpha_1}(t)\perp\left(BM(t)\right)\right)$;

vector $\left(\vec{\mathbf{V}}_{r\alpha_2}(t)[m/s]\right)$ is parallel to the horizontal plane ($x_2O_2y_2$); where vector $\left(\vec{\mathbf{V}}_{r\alpha_2}(t)\perp\left(O_1M_1(t)\right)\right)$;

$$\left(\left|\vec{\mathbf{V}}_{r\alpha_2}(t)\right| = V_{r\alpha_2}(t) = \left(\left(\dot{\alpha}_2(t)\right)\cdot\left(O_1M_1(t)\right)\right)\right.$$

$$\left.= \left(\left(\dot{\alpha}_2(t)\right)\cdot\left(l(t)\cdot\sin(\alpha_1(t))\right)\right)\left[\frac{m}{s}\right];\right.$$

velocity $\left(\vec{\mathbf{V}}_{\mathbf{e}}(t)[m/s]\right)$ of portable transportation is parallel to the horizontal plane ($x_2O_2y_2$);

vector $\left(\vec{\mathbf{V}}_{\mathbf{e}}(t)\perp\left(O_2M_1(t)\right)\right)$;

$$\left(\left|\vec{\mathbf{V}}_{\mathbf{e}}(t)\right| = V_e(t) = \left(O_2M_1(t)\right)\cdot\left(\dot{\varphi}_e(t)\right)[m/s]\right);$$

vector $\left(\vec{\mathbf{V}}_{r\alpha_2}(t)[m/s]\right)$ is parallel to the horizontal plane ($x_2O_2y_2$); where vector $\left(\vec{\mathbf{V}}_{r\alpha_2}(t)\perp\left(O_1M_1(t)\right)\right)$;

($x_2O_2y_2z_2$) – fixed inertial reference system;

($x_1O_1y_1z_1$) – movable noninertial reference frame.

The interrelation between the relative spherical ($\alpha_1(t)$; $\alpha_2(t)$) and the relative Cartesian coordinates ($x_1(t)$; $y_1(t)$; $z_1(t)$; $l(t)$) in Figure 1 is as follows:

$$O_1M_1(t) = l(t)\cdot\sin(\alpha_1(t));$$
$$x_1(t) = O_1M_1(t)\cdot\cos(\alpha_2(t)) = l(t)\cdot\sin(\alpha_1(t))\cdot\cos(\alpha_2(t));$$
$$y_1(t) = O_1M_1(t)\cdot\sin(\alpha_2(t)) = l(t)\cdot\sin(\alpha_1(t))\cdot\sin(\alpha_2(t));$$
$$z_1(t) = l_0 - l(t)\cdot\cos(\alpha_1(t)).$$

The position of the payload (M) attached to the crane boom (DB) can be described with 5 (five) dependent coordinates:

$$\vec{\mathbf{p}}(t) = \left[\varphi_e(t), l(t), x_1(t), y_1(t), z_1(t)\right];$$

where

$\vec{\mathbf{p}}(t)$ – vector, determining the position of the payload (M),

($x_1(t)[m]$, ($y_1(t)[m]$, ($z_1(t)[m]$) – the relative Cartesian coordinates of the payload (M) in the non-inertial coordinate system associated with the end (B) of the boom (DB).

The relative coordinates of the payload (M) and the length of the cable ($l(t)[m]$) are connected by the following coupling equation:

$$\Phi = \Phi\left(x_1(t), y_1(t), z_1(t), l(t), t\right);$$
$$\Phi = \sqrt{x_1^2(t) + y_1^2(t) + \left(l_0 - z_1(t)\right)^2} - l(t) = 0,$$

where ($l_0[m]$) – initial length of the cable.

A system of differential equations, describing the behavior of a dynamic controlled crane system in relative coordinates ($x_1(t)[m]$), ($y_1(t)[m]$), and ($z_1(t)[m]$):

$$\begin{aligned}
&m\cdot\left(\frac{d^2(x_1(t))}{dt^2}\right) = -N(t)\cdot\left(\frac{(x_1(t))}{(l(t))}\right) + \\
&m\cdot\left(\frac{d(\varphi_e(t))}{dt}\right)^2\cdot(x_1(t)) + m\cdot\left(\frac{d^2(\varphi_e(t))}{dt^2}\right)\cdot(R + (y_1(t))) + \\
&2\cdot m\cdot\left(\frac{d(\varphi_e(t))}{dt}\right)\cdot\left(\frac{d(y_1(t))}{dt}\right); \qquad (1)\\
&m\cdot\left(\frac{d^2(y_1(t))}{dt^2}\right) = -N(t)\cdot\left(\frac{(y_1(t))}{(l(t))}\right) + \\
&m\cdot\left(\frac{d(\varphi_e(t))}{dt}\right)^2\cdot(R + (y_1(t))) - m\cdot\left(\frac{d^2(\varphi_e(t))}{dt^2}\right)\cdot(x_1(t)) -
\end{aligned}$$

$$2\cdot m\cdot\left(\frac{d(\varphi_e(t))}{dt}\right)\cdot\left(\frac{d(x_1(t))}{dt}\right); \tag{2}$$

$$m\cdot\left(\frac{d^2(z_1(t))}{dt^2}\right)=(-m\cdot g)+N(t)\cdot\left(\frac{(l_0-z_1(t))}{(l(t))}\right); \tag{3}$$

$$J_1\cdot\left(\frac{d^2(l(t))}{dt^2}\right)=r_w^2\cdot N(t)-M_w(t)\cdot r_w; \tag{4}$$

$$J_2\cdot\left(\frac{d^2(\varphi_e(t))}{dt^2}\right)=M(t)-R\cdot N(t)\cdot\left(\frac{(x_1(t))}{(l(t))}\right), \tag{5}$$

coupling equation:

$$l^2(t)=\left(x_1^2(t)+y_1^2(t)+(l_0-z_1(t))^2\right), \tag{6}$$

where

($l(t)[m]$) – variable cable length;

($m[kg]$) – load weight;

($J_1[\text{kg}\cdot\text{m}^2]$) – moment of inertia of the winch;

($J_2[\text{kg}\cdot\text{m}^2]$) – moment of inertia of the tower;

($R[m]$) – boom (DB) radius;

($r_w[m]$) – winch radius;

($l_0[m]$) – distance (BO_1) from the point (B) of suspension to the base (O_1) of the tower;

($M(t)$ $[N\cdot m]$) – electromagnetic torque developed by the drive motor of the tower;

($M_w(t)$ $[N\cdot m]$) – electromagnetic torque developed by the winch drive motor;

($N(t)[N]$) – tension of the cable.

Equations (1) – (3) were obtained in our previous work (A. V. Perig, A. N. Stadnik, et al., 2014) [12–13].

Equation 4 is the equation of rotational motion of the winch.

The length of the cable ($l(t)[m]$) is related to the angle $\theta(t)$ of winch rotation by the following expression:

$$l(t)=r_w\cdot\theta(t)$$

Equation 5 is the equation of the rotational motion of the crane boom.

Because the electromagnetic torque developed by the electric motor is proportional to the armature current, then:

$$\begin{cases} M(t)=k_t\cdot i(t); \\ M_w(t)=k_{wt}\cdot i_w(t), \end{cases} \tag{7}$$

where

($i(t)$; $i_w(t)[A]$)– currents of armatures of electric motors of a tower and a winch respectively;

$\left(k_t; k_{wt}\left[\frac{N\cdot m}{A}\right]\right)$ – proportionality coefficients.

The voltages on the armature windings are determined by the relations:

$$\begin{cases} u_e(t)=e(t)+R_e\cdot i(t); \\ u_w(t)=e_w(t)+R_w\cdot i_w(t), \end{cases} \tag{8}$$

where

($u_e(t)$; $u_w(t)[V]$) – voltages on the winding of the armature of the electric motor of the tower and the winch respectively;

(R_e; $R_w[Ohm]$) – active armatures resistance,

($e(t)$; $e_w(t)[V]$)(e(t)) – electric-motion force (emf) armatures.

The emf of the armatures are related to the angular velocity of rotation by the relations:

$$\begin{cases} e(t)=k_e\cdot\omega(t); \\ e_w(t)=k_{ew}\cdot\omega_w(t). \end{cases} \tag{9}$$

Using relations (7) – (9), equations (4) and (5) can be rewritten in the form:

$$J_1\cdot\left(\frac{d^2(l(t))}{dt^2}\right)=r_w^2\cdot N(t)-$$
$$\left(\frac{k_{wt}\cdot r_w}{R_w}\right)\cdot u_w(t)+\left(\frac{k_{wt}\cdot k_{ew}}{R_w}\right)\cdot\left(\frac{d(l(t))}{dt}\right); \tag{10a}$$

$$J_2\cdot\left(\frac{d^2(\varphi(t))}{dt^2}\right)=\left(\frac{k_t\cdot u_e(t)}{R_e}\right)-$$
$$\left(\frac{k_t\cdot k_e}{R_e}\right)\cdot\left(\frac{d(\varphi_e(t))}{dt}\right)-R\cdot N(t)\cdot\left(\frac{(x_1(t))}{(l(t))}\right). \tag{10b}$$

It is possible to express $N(t)$ through $x_1(t)$, $y_1(t)$, $l(t)$ and their derivatives.

From equation (3) we get:

$$N(t)=\left(\frac{(m\cdot l(t))}{(l_0-z_1(t))}\right)\cdot\left(g+\left(\frac{d^2(z_1(t))}{dt^2}\right)\right); \tag{7}$$

Table 1. The first algebraic expression for cable tension force N = N(t) [N].

$$N(t)=\left(\frac{(m\cdot l(t)\cdot g)}{\left(\sqrt{(l(t))^2-(x_1(t))^2-(y_1(t))^2}\right)}\right)+$$
$$\left(\frac{(m\cdot l(t))}{\left((l(t))^2-(x_1(t))^2-(y_1(t))^2\right)}\right)\cdot\left(\left(\frac{d(x_1(t))}{dt}\right)^2+x_1(t)\cdot\left(\frac{d^2(x_1(t))}{dt^2}\right)+\left(\frac{d(y_1(t))}{dt}\right)^2+y_1(t)\cdot\left(\frac{d^2(y_1(t))}{dt^2}\right)-\left(\frac{d(l(t))}{dt}\right)^2-l(t)\cdot\left(\frac{d^2(l(t))}{dt^2}\right)\right)+$$
$$\left(\frac{(m\cdot l(t))}{\left(\left((l(t))^2-(x_1(t))^2-(y_1(t))^2\right)^2\right)}\right)\cdot\left((x_1(t))^2\cdot\left(\frac{d(x_1(t))}{dt}\right)^2+(y_1(t))^2\cdot\left(\frac{d(y_1(t))}{dt}\right)^2+(l(t))^2\cdot\left(\frac{d(l(t))}{dt}\right)^2\right)+$$
$$\frac{(2\cdot m\cdot l(t))}{\left((l(t))^2-(x_1(t))^2-(y_1(t))^2\right)^2}\cdot\left(x_1(t)\cdot y_1(t)\cdot\left(\frac{d(x_1(t))}{dt}\right)\cdot\left(\frac{d(y_1(t))}{dt}\right)-x_1(t)\cdot l(t)\cdot\left(\frac{d(x_1(t))}{dt}\right)\cdot\left(\frac{d(l(t))}{dt}\right)-y_1(t)\cdot l(t)\cdot\left(\frac{d(y_1(t))}{dt}\right)\cdot\left(\frac{d(l(t))}{dt}\right)\right)$$

Table 2. Algebraic expressions for load velocity ($d(z_1(t))/dt$) [m/s] and load acceleration ($d^2(z_1(t))/dt^2$) [m/s^2].

$\left(\frac{d(z_1(t))}{dt}\right)=\frac{\left(x_1(t)\cdot\left(\frac{d(x_1(t))}{dt}\right)+y_1(t)\cdot\left(\frac{d(y_1(t))}{dt}\right)-l(t)\cdot\left(\frac{d(l(t))}{dt}\right)\right)}{\left(\sqrt{(l(t))^2-(x_1(t))^2-(y_1(t))^2}\right)}$
$\left(\frac{d^2(z_1(t))}{dt^2}\right)=\frac{1}{\left(\sqrt{(l(t))^2-(x_1(t))^2-(y_1(t))^2}\right)}\times$ $\times\left(\left(\frac{d(x_1(t))}{dt}\right)^2+x_1(t)\cdot\left(\frac{d^2(x_1(t))}{dt^2}\right)+\left(\frac{d(y_1(t))}{dt}\right)^2+y_1(t)\cdot\left(\frac{d^2(y_1(t))}{dt^2}\right)-\right.$ $\left.\left(\frac{d(l(t))}{dt}\right)^2-l(t)\cdot\left(\frac{d^2(l(t))}{dt^2}\right)+\frac{\left(x_1(t)\cdot\left(\frac{d(x_1(t))}{dt}\right)+y_1(t)\cdot\left(\frac{d(y_1(t))}{dt}\right)-l(t)\cdot\left(\frac{d(l(t))}{dt}\right)\right)^2}{\left((l(t))^2-(x_1(t))^2-(y_1(t))^2\right)}\right)$

Detailed expression (7) is shown in Table 1. The following auxiliary expressions in Table 2 were used for derivation of expression in Table 1:

$$l_0-z_1(t)=\sqrt{(l(t))^2-(x_1(t))^2-(y_1(t))^2}\ .$$

2.2 Formulation of optimal control problem

It is possible to introduce the following phase variables:

$$p_1(t)=x_1(t);$$
$$p_2(t)=\frac{d(x_1(t))}{dt};$$
$$p_3(t)=y_1(t);$$
$$p_4(t)=\frac{d(y_1(t))}{dt};$$
$$p_5(t)=l(t);$$
$$p_6(t)=\frac{d(l(t))}{dt};$$
$$p_7(t)=\varphi(t);$$
$$p_8(t)=\frac{d(\varphi(t))}{dt}.$$

It is possible to introduce the following control variables:

$u_e(t)$
and
$u_w(t)$.

The optimum performance problem for the above dynamic controlled crane system is set as follows:
find such control

$u_e(t)$
and
$u_w(t)$,

that gives a minimum of the functional

$$J=t_f$$

under the following restrictions:

$$\left(\frac{d(p_1(t))}{dt}\right)=p_2(t);$$

$$\left(\frac{d(p_2(t))}{dt}\right)=-\left(\frac{N(t)}{m}\right)\cdot\left(\frac{p_1(t)}{p_5(t)}\right)+\left(\left(p_8^2(t)\right)\cdot p_1(t)\right)+$$
$$\left(\frac{d(p_8(t))}{dt}\right)\cdot(R+p_3(t))+(2\cdot p_8(t)\cdot p_4(t));$$

$$\left(\frac{d(p_3(t))}{dt}\right)=p_4(t);$$

$$\left(\frac{d(p_4(t))}{dt}\right)=-\left(\frac{N(t)}{m}\right)\cdot\left(\frac{p_3(t)}{p_5(t)}\right)+\left(\left(p_8^2(t)\right)\cdot(R+p_3(t))\right)-$$
$$\left(\frac{d(p_8(t))}{dt}\right)\cdot p_1(t)-(2\cdot p_8(t)\cdot p_2(t));$$

$$\left(\frac{d(p_5(t))}{dt}\right)=p_6(t);$$

$$\frac{d(p_6(t))}{dt}=\left(\frac{r_w^2}{J_1}\right)\cdot N(t)-$$
$$\left(\frac{k_{wt}\cdot r_w}{R_w\cdot J_1}\right)\cdot u_w(t)+\left(\frac{k_{wt}\cdot k_{ew}}{R_w\cdot J_1}\right)\cdot p_6(t);$$

$$\frac{d(p_7(t))}{dt}=p_8(t);$$

$$\left(\frac{d(p_8(t))}{dt}\right)=\left(\frac{k_t}{R_e\cdot J_2}\right)\cdot u_e(t)-$$
$$\left(\frac{k_t\cdot k_e}{R_e\cdot J_2}\right)\cdot p_8(t)-\left(\frac{R}{J_2}\right)\cdot\left(\frac{p_1(t)}{p_5(t)}\right)\cdot N(t).$$

Using notation

$$Q=Q(p_1,\,p_3,\,p_5)=\frac{1}{\left(\sqrt{p_5^2(t)-p_1^2(t)-p_3^2(t)}\right)},$$

now expression for $N = N(t)$ from the Table 1 is written in the Table 3.

Table 3. The second algebraic expression for cable tension force N = N(t) [N].

$$
\begin{aligned}
&N(t)=(m\cdot g\cdot p_5(t)\cdot Q)+\\
&(m\cdot p_5(t)\cdot(Q^2))\cdot\left((p_2(t))^2+\left(p_1(t)\cdot\left(\frac{d(p_2(t))}{dt}\right)\right)+(p_4(t))^2+\left(p_3(t)\cdot\left(\frac{d(p_4(t))}{dt}\right)\right)-(p_6(t))^2-\left(p_5(t)\cdot\left(\frac{d(p_6(t))}{dt}\right)\right)\right)+\\
&(m\cdot p_5(t)\cdot(Q^4))\cdot(((p_1(t))^2)\cdot((p_2(t))^2))+(((p_3(t))^2)\cdot((p_4(t))^2))+(((p_5(t))^2)\cdot((p_6(t))^2))+\\
&(2\cdot m\cdot p_5(t)\cdot(Q^4))\cdot((p_1(t)\cdot p_3(t)\cdot p_2(t)\cdot p_4(t))-(p_1(t)\cdot p_5(t)\cdot p_2(t)\cdot p_6(t))-(p_3(t)\cdot p_5(t)\cdot p_4(t)\cdot p_6(t)))
\end{aligned}
$$

There are not only phase variables but also their derivatives in $N = N(t)$ expression in the Table 3.

Initial conditions are as follows:

$p_1(0)=0$;
$p_2(0)=0$;
$p_3(0)=0$;
$p_4(0)=0$;
$p_5(0)=l_0$;
$p_6(0)=0$;
$p_7(0)=0$;
$p_8(0)=0$.

Final conditions are as follows:

$p_1(t_f)=0$;
$p_2(t_f)=0$;
$p_3(t_f)=0$;
$p_4(t_f)=0$;
$p_5(t_f)=l_f$;
$p_6(t_f)=0$;
$p_7(t_f)=\pi$;
$p_8(t_f)=0$.

Constraints on the control variables are as follows:

$$
\begin{cases}
|u_e(t)|\le u_{eb};\\
|u_w(t)|\le u_{wb}.
\end{cases}
$$

Constraints on the amount of swing are given in the form:

$$p_1^2(t)+p_3^2(t)\le\varepsilon\ ,$$

where ε – allowable amount of payload swing.

The numerical solution of this problem (Figs. 2 – 18) was obtained using the Optimica application [8-9, 14-15, 23-25]. Optimica is the extension of JModelica.org, which solves the optimal control problem. Optimica obtains solutions of the optimal control problem by its reduction to a nonlinear programming problem (Benson et al. (2006), [24]). The use of JModelica.org with Optimica extension [8,9,14,15,23-25] has made it possible to easily solve the problem of optimal control [26].

3. NUMERICAL SOLUTION RESULTS OF THE OPTIMAL PERFORMANCE PROBLEM

The aim of our numerical simulation was to identify the effect of the permissible value of payload swing on the optimal performance problem solution.

Modeling results for the case of no restriction on the payload swaying value are shown in Figures 2 – 8.

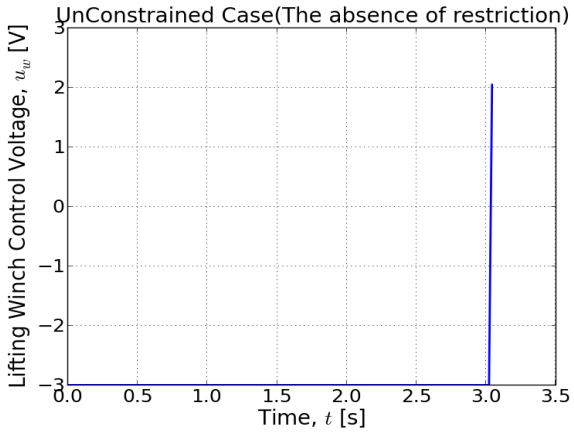

Figure 2. Optimal control voltage $u_w = u_w(t)$ [V] for the winch electric drive in the unconstrained case for the absence of restrictions

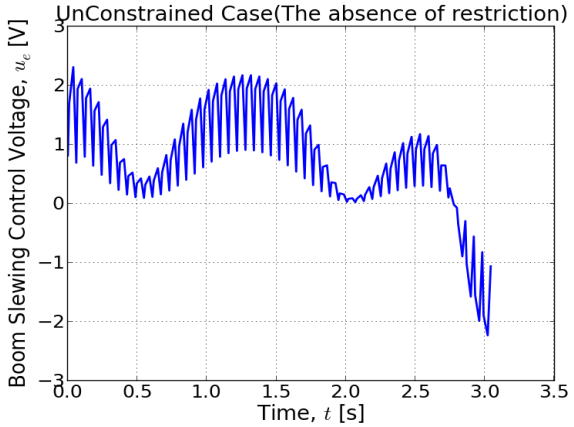

Figure 3. Optimal control voltage $u_e = u_e(t)$ [V] for the boom-rotating tower electric drive in the unconstrained case for the absence of restrictions

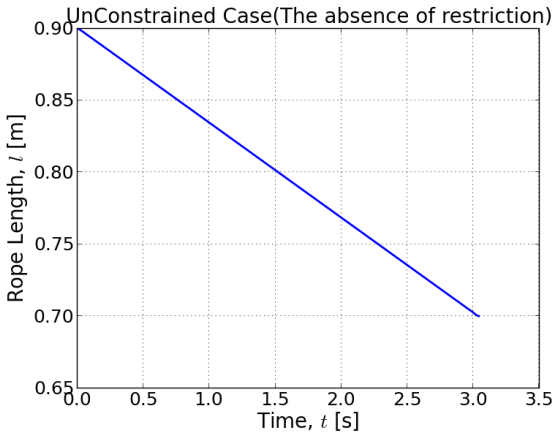

Figure 4. Graph of cable length changing L = L(t) [m] in the dynamic crane system under optimal control without constraints on the payload swaying value

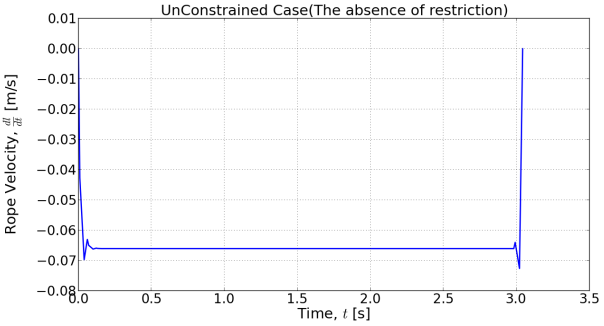

Figure 5. Graph of cable length changing velocity d(L)/dt = d(L(t))/dt [m/s] in the dynamic crane system under optimal control without constraints on the payload swaying value

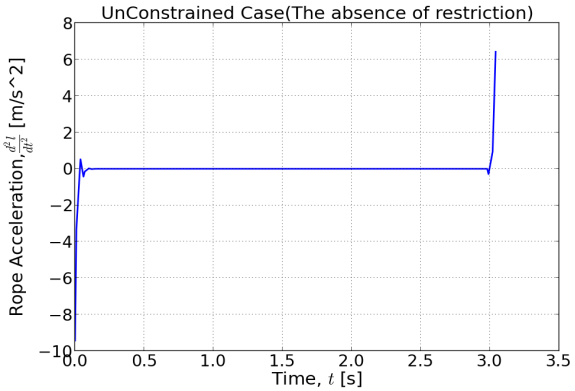

Figure 6. Graph of cable length changing acceleration $d^2(L)/dt^2 = d^2(L(t))/dt^2$ [m/s^2] in the dynamic crane system under optimal control without constraints on the payload swaying value

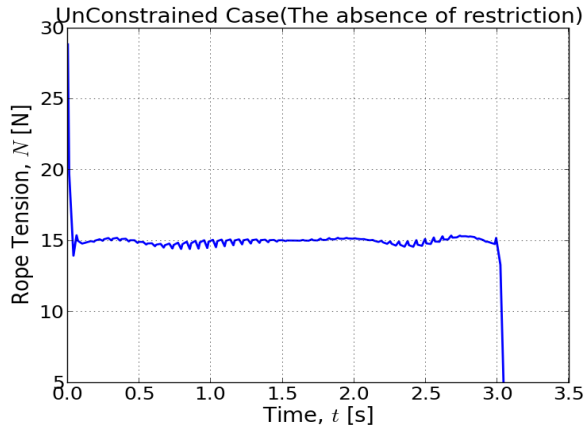

Figure 7. Optimal control rope tension N = N(t) [N] in the unconstrained case for the absence of restrictions

Figures 9 – 15 show modeling results in the case of the restriction

$$p_1^2(t) + p_3^2(t) \le \varepsilon$$

on the payload swaying value.

Absolute trajectory graphics of the payload are presented below (Figures 8, 15, 17).

Figures 2 – 18 are obtained with the following numerical values of the parameters: where

$$m = 1.5\,[kg];$$

$$k_{wt} = k_{ew} = 0.0261\left[\frac{N \cdot m}{A}\right];$$

$$r_w = 0.15\,[m];$$

$$J_1 = 2.58 \cdot 10^{-5}\,[kg \cdot m^2];$$

$$J_2 = 5\,[kg \cdot m^2];$$

$$R_e = 11.4\,[Ohm];$$

$$R_w = 7.1\,[Ohm];$$

$$R = 0.73\,[m];$$

$$k_t = k_e = 0.119\left[\frac{N \cdot m}{A}\right];$$

$$l_0 = 0.9\,[m];$$

$$l_f = 0.7\,[m];$$

$$u_{eb} = u_{wb} = 3\,[V];$$

$$\varepsilon = 0.01\,[m^2].$$

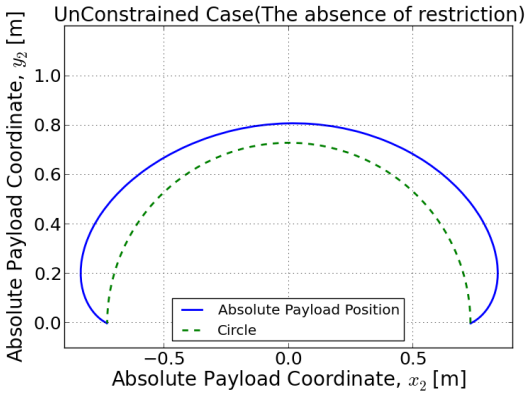

Figure 8. Absolute trajectory $y_2 = y_2(x_2)$ [m] of the payload in the case of optimal control without the constraint on the payload swaying value

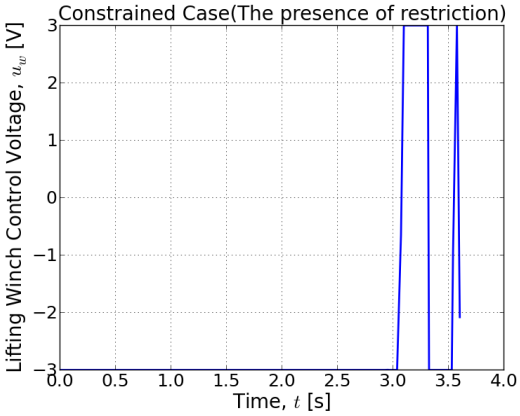

Figure 9. Optimal control voltage $u_w = u_w(t)$ [V] for the winch electric drive in the constrained case for the presence of restrictions

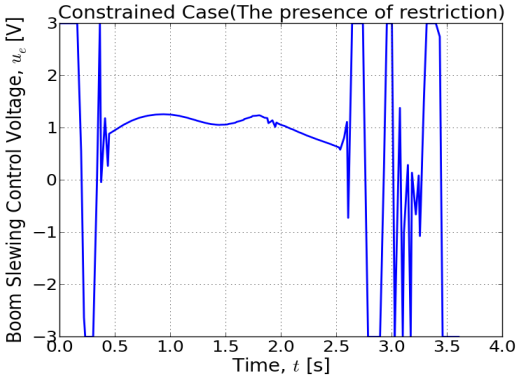

Figure 10. Optimal control voltage $u_e = u_e(t)$ [V] for the boom-rotating tower electric drive in the constrained case for the presence of restrictions

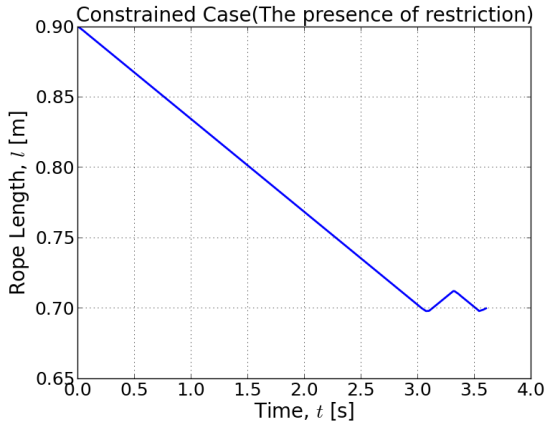

Figure 11. Graph of cable length changing L = L(t) [m] in the dynamic crane system under optimal control with constraints on the payload swaying value

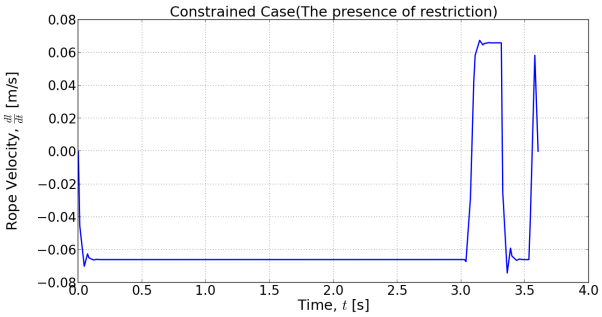

Figure 12. Graph of cable length changing velocity d(L)/dt = d(L(t))/dt [m/s] in the dynamic crane system under optimal control with constraints on the payload swaying value

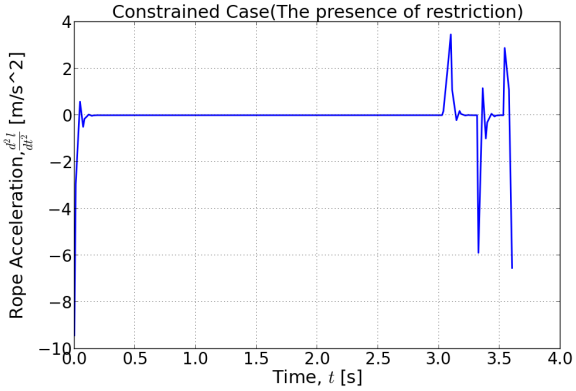

Figure 13. Graph of cable length changing acceleration $d^2(L)/dt^2 = d^2(L(t))/dt^2$ [m/s^2] in the dynamic crane system under optimal control with constraints on the payload swaying value

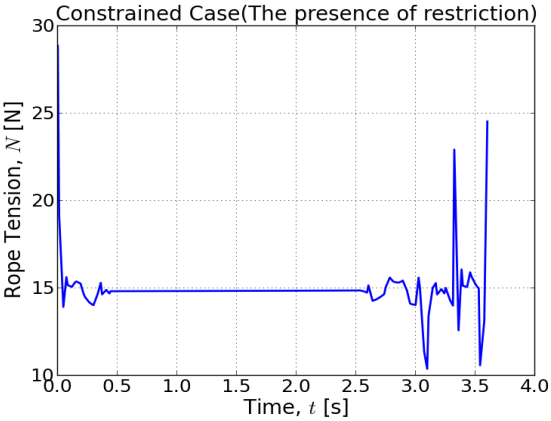

Figure 14. Optimal control rope tension N = N(t) [N] in the constrained case for the presence of restrictions

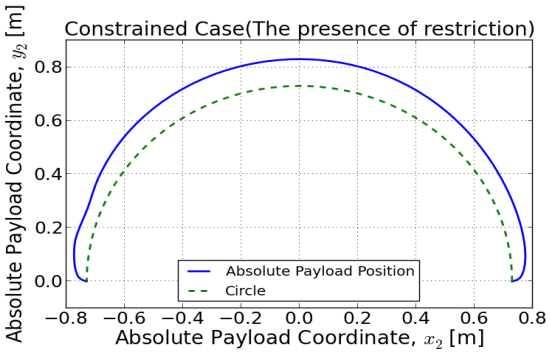

Figure 15. Absolute trajectory $y_2 = y_2(x_2)$ [m] of the payload in case of optimal control with restrict on the payload swaying value

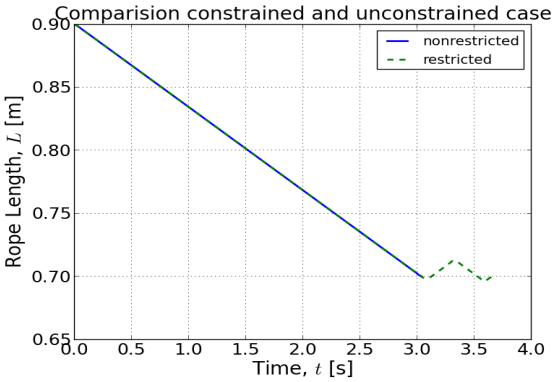

Figure 16. Complex graph of cable length changing L = L(t) [m] in the dynamic crane system under optimal control with and without constraints on the payload swaying value

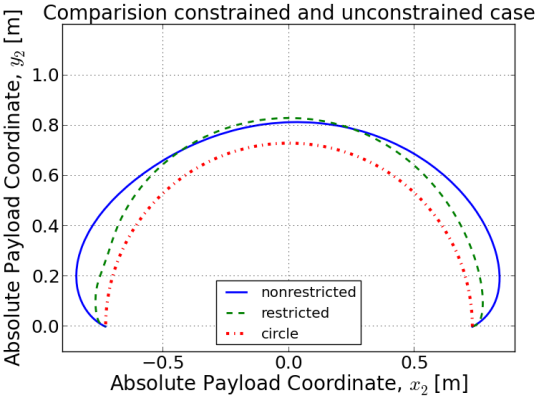

Figure 17. Complex graph of absolute payload trajectory $y_2 = y_2(x_2)$ [m] in the dynamic crane system under optimal control with and without constraints on the payload swaying value

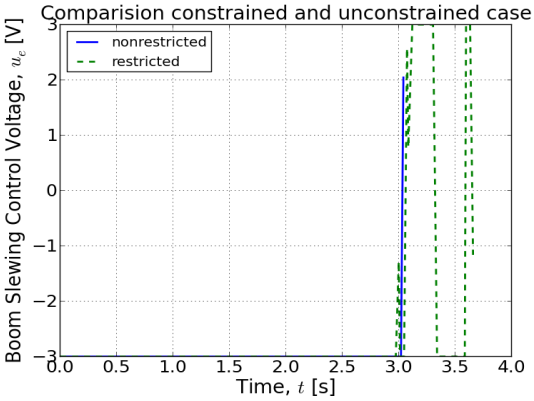

Figure 18. Complex graph of optimal control voltage $u_e = u_e(t)$ [V] with and without constraints on the payload swaying value

There are comparisons below of some characteristics of the dynamic crane system under optimal control with and without constraints on the payload swaying value (Figures 16 – 18).

4. DISCUSSIONS

The damping of the oscillations of the load is accomplished by the control torque. The simulation results show that increasing the torque developed by the electric motor moves the load quickly to the desired position. However, such action leads to the appearance of overshoot in the controllable parameter "cable length" (Figures 4, 14, 16), and also leads to overloads in the subsystem "crane boom – suspension – cable". In the case of no constraint on the module of the amplitude of the load swing during transportation, the overshoot of the controlled parameter "cable length" is not observed (Figure 4). When the allowable control torque is increased, overshoot of the parameter "cable length" occurs earlier. However, such changing of the torque increases the performance of the entire crane system (Figure 1).

From the obtained graphs (Figure 10) it is evident that during half a second from the beginning of the movement a steady state is reached. Then the system behaves in accordance with the specified requirements when the control torque is non-zero constant. At the end of the turn phase, in order to ensure that the system is in a state of static equilibrium, it is necessary for the load to arrive at the final point of the trajectory with zero speed (Figures 8, 15, 17). Such a constraint on the final load speed is rigid. Therefore, in future studies, it is planned to specify a final velocity as a certain near-zero value.

The system transition from dynamic equilibrium to static equilibrium is accompanied by switching control moments (relay mode) (Figures 9, 10, 18). For the model without the constraint on the amount of load swing this transition takes about a half a second (Figures 2 – 7). For the model with the constraint the transition takes about a second (Figures 9 – 14).

A special study interest is the graph of the optimal torque control of the crane boom (Figures 3, 10). In the absence of a restriction on the value of the load swing, the function $u_e(t)[V]$ has a pronounced oscillatory character (Figure 3). This is most likely due to the natural frequencies of the crane system and its properties.

To determine the natural frequencies of a system, a consistent reduction in the number of degrees of freedom is required.

It is possible to make a qualitative comparison between the numerical simulation results by Kostikov et al., which were derived in the present study (Figures 2 – 18), and the well-known computational results, which were previously found and reported in the well-known paper by Abdel-Rahman & Nayfeh (2002) [2].

At the first step we will make an estimation of the numerical value of the dimensionless coefficient of the length scale through a comparison of the numerical values of the initial cable length l_0 for both boom crane models. It is written at p. 263 of paper [2] that $l_{0\,(\text{Abdel-Rahman \& Nayfeh})} = 89$ [ft]. The initial value of cable length in our paper is equal to $l_{0\,(\text{Kostikov et al.})} = 0.9$ [m]. Therefore, it is possible to introduce a new length scale dimensionless coefficient for the length of the crane rope, attached to the boom tip, as $l_{scale} = (l_{0\,(\text{Abdel-Rahman \& Nayfeh})})/(l_{0\,(\text{Kostikov et al.})})$. The numerical value of this dimensionless quantity l_{scale} is $l_{scale} = (89\ [\text{ft}])/(0.9\ [\text{m}]) \approx 30.141$.

At the second step we will make an estimation of the numerical value of the velocity scale dimensionless coefficient through a comparison of the numerical values of the payload lifting velocity V_l for both boom crane models. It is written at p. 264 of paper [2] that $V_{l\,(\text{Abdel-Rahman \& Nayfeh})} = 1.5$ [ft/s]. The computational 2D plots for payload lifting velocity, which were derived in the present paper by Kostikov et al., are shown in our graphical plots in Figures 5 and 12. These plots yield that our numerical value of the payload lifting velocity is $V_{l\,(\text{Kostikov et al.})} = 0.065$ [m/s]. Therefore, it is possible to introduce a new payload velocity scale dimensionless coefficient for the linear velocity of the lifting of the crane rope, attached to the boom tip, as $V_{l(scale)} = (V_{l\,(\text{Abdel-Rahman \& Nayfeh})})/(V_{l\,(\text{Kostikov et al.})})$. The numerical value of this dimensionless quantity $V_{l\,(\text{scale})}$ is $V_{l\,(\text{scale})} = (1.5\ [\text{ft/s}])/(0.065\ [\text{m/s}]) \approx 7.034$.

At the third step we take into account that the scaling condition for the kinematic similarity yields that $V_{l\,(\text{scale})} = (l_{\text{scale}})/(t_{\text{scale}})$, where the new dimensionless quantity t_{scale} is the timescale factor, which can be estimated as $t_{\text{scale}} = (l_{\text{scale}})/(V_{l\,(\text{scale})})$. The previous estimations yield the following numerical value of this dimensionless quantity as $t_{scale} \approx (30.141)/(7.034) \approx 4.285$.

At the fourth step we recall the following expression between the dimensionless quantities of time scale t_{scale} and frequency scale ω_{scale} in the form of $t_{\text{scale}} = 1/\omega_{\text{scale}}$ and $\omega_{\text{scale}} = 1/t_{\text{scale}} \approx (7.034)/(30.141) \approx 0.233$. Additionally, the same dimensionless quantity for frequency scale can be standardly determined through the following expression:

$$\omega_{\text{scale}} = (\omega_{\,(\text{Abdel-Rahman \& Nayfeh})})//(\omega_{(\text{Kostikov et al.})}).$$

It is written at p. 262 of paper [2] that the numerical value of the excitation frequency is equal to $\omega_{\,(\text{Abdel-Rahman \& Nayfeh})} = 0.601$ [rad/s]. It is possible to find the following algebraic expression $\omega_{\,(\text{Kostikov et al.})} = (\omega_{\,(\text{Abdel-Rahman \& Nayfeh})})/(\omega_{\text{scale}})$ for the calculation of the numerical value of the excitation frequency $\omega_{\,(\text{Kostikov et al.})}$ in our case for the present problem by Kostikov et al.:

$$\omega_{\,(\text{Kostikov et al.})} \approx 0.601\ [\text{rad/s}])/(0.233) \approx 2.579\ [\text{rad/s}].$$

At the fifth step we take into account that the dimensionless value of the linear acceleration scale a_{scale} for linear motion of a rope-lifted, boom-transported payload is determined as $a_{\text{scale}} = (V_{l\,(\text{scale})})/(t_{\text{scale}})$. The numerical value of a_{scale} in our case is as follows: $a_{\text{scale}} \approx (7.034)/(4.285) \approx 1.642$.

At the sixth step we address concepts of the dynamic similarity theory. It is well known that the mass scale dimensionless parameter can be calculated with the following expression: $m_{\text{scale}} = (\rho_{\text{scale}})\bullet[(l_{\text{scale}})^3]$, where ρ_{scale} is the mass density scale dimensionless parameter. For simplicity of further comparison, we assume that ρ_{scale} has a unity value $\rho_{\text{scale}} = 1$. Then, for a numerical value of the dimensionless mass scaling factor we have $m_{\text{scale}} = [(l_{\text{scale}})^3] \approx (30.141)^3 \approx 27382.492$.

At the seventh step we are ready to determine the algebraic equation for the force scale F_{scale} dimensionless parameter as $F_{scale} = (m_{scale})\cdot(a_{scale})$. The numerical value of F_{scale} is as follows: $F_{scale} \approx (27382.492)\cdot(1.642) \approx 44962.052$. We can additionally check the correctness of this estimated numerical value of the force scale F_{scale} dimensionless parameter through the use of the following alternative algebraic expression $F_{scale1} = (\rho_{scale})\cdot[(l_{scale})^2]\cdot[(V_{l\,(scale)})^2]$. In our case we have the following numerical value of $F_{scale1} \approx [(30.141)^2]\cdot[(7.034)^2] \approx 44949$. It is obvious that F_{scale} almost coincides with the previous numerical value of F_{scale1}.

At the eighth step we can make an approximate estimate of the numerical value of the scale of the non-reduced dimensionless damping coefficient β_{scale} through the use of the following dimensionless expression: $F_{scale} = (\beta_{scale})\bullet(V_{l\,(scale)})$. The algebraic expression for the scale of the β_{scale} is the solution of the previous equation, which yields $(\beta_{scale}) = (F_{scale})/(V_{l\,(scale)})$. The numerical value of the β_{scale} is as follows: $(\beta_{scale}) \approx (44962.052)/(7.034) \approx 6392.243$. In order to make the bridge between this estimation for the scale of the non-reduced dimensionless damping coefficient β_{scale} and p. 258 of the paper [2], we introduce a new dynamic similarity-based dimensionless expression for the scale of the reduced, normalized and normed dimensionless damping coefficient μ_{scale} through the use of the following dimensionless expression: $(\mu_{scale}) = (\beta_{scale})/(m_{scale})$, which yields $(\mu_{scale}) \approx (6392.243)/(27382.492) \approx 0.233$. From another viewpoint, the scale of the reduced, normed and normalized dimensionless damping coefficient μ_{scale} can be calculated as $(\mu_{scale}) = (\mu_{(Abdel\text{-}Rahman\ \&\ Nayfeh)})/(\mu_{(Kostikov\ et\ al.)})$. It is written on p. 262 of paper [2] that the numerical value of the reduced, normalized and normed linear damping coefficient is equal to $\mu_{(Abdel\text{-}Rahman\ \&\ Nayfeh)} = 0.01$. The following algebraic expression $\mu_{(Kostikov\ et\ al.)} = (\mu_{(Abdel\text{-}Rahman\ \&\ Nayfeh)})/(\mu_{scale})$ can be used for the calculation of the numerical value of the reduced, normalized and normed linear damping coefficient $\mu_{(Kostikov\ et\ al.)}$ in our case for the present problem by Kostikov et al.: $\mu_{(Kostikov\ et\ al.)} \approx (0.01)/(0.233) \approx 0.043$.

These kinematic and dynamic similarity-based engineering estimations expand our understanding of the authors-derived results of numerical simulations in the present paper, shown in computational Figures 2 – 18.

5. CONCLUSION

Computational plots of time dependencies of control voltages ($u_e(t)$; $u_w(t)[V]$) in Figures 2, 3, 9, 10 have a stick-slip nature. This fact allows us to make a conclusion that our numerical solution for the optimal control voltages really fits the Bang-Bang type of optimal control within some specific time intervals.

Even in the simplest case of no restrictions, our problem is not reduced to a classical optimal control problem for Pontryagin's type, in which the principle of Pontryagin's maximum is proved.

It is tied to the fact, that rope tension force $N = N(t)$ depends on not only phase variables, but also on their derivatives (Figures 7, 14). The cable tension force $N = N(t)$ is the internal force of the mechanical system "boom crane – payload". The algebraic expressions for $N = N(t)$ are listed in the Table 1 and Table 3. Expressions in the Table 1 and Table 3 show that the rope tension force $N = N(t)$ is a non-linear function of the first derivatives of the phase variables. Therefore, it is very difficult to express all first derivatives with the phase and control variables.

In order to be able to apply Pontryagin's (Pontriagin's) maximum principle to the present optimization problem, it is necessary to express the studied dynamic system in the form

$$\left(\frac{d(x(t))}{dt}\right) = f(x(t), u(t)),$$

where $x(t)$ is the phase variable and $u(t)$ is the control variable. However, it is very complex assignment to express the system in this form. Therefore, it is very challenging assignment to directly apply Pontryagin's (Pontriagin's) maximum principle for our dynamic system in the present research. That is why our dynamic system in the staging of the optimal control problem, does not satisfy conditions for which Pontryagin's principle of maximum is proved. Consequently, qualitative analysis of our optimal control problem using Pontryagin's principle of maximum requires research data which is beyond the scope of this research. Addressing this problem will be a matter of further study by the authors.

REFERENCES

[1] Abe, A.: Non-linear control technique of a pendulum via cable length manipulation: Application of particle swarm optimization to controller design, FME Transactions, Vol. 41, No. 4, pp. 265-270, 2013.

[2] Abdel-Rahman, E.M., Nayfeh, A.H.: Pendulation reduction in boom cranes using cable length manipulation, Nonlinear Dynamics, Vol. 27, No. 3, pp. 255-269, 2002, doi:10.1023/A:1014437225984.

[3] Abdel-Rahman, E.M., Nayfeh, A.H., Masoud, Z.N.: Dynamics and control of cranes: A review, Journal of Vibration and Control, Vol. 9, No. 7, pp. 863-908, 2003, doi:10.1177/1077546303009007007.

[4] Aleynik, V., Repin, S. and Rulis, C.: Assessment of the Coriolis force impact on the operation of the tower crane swing mechanism, Architecture and Engineering, Vol. 1, No. 4, pp. 3-6, 2016, doi:10.23968/2500-0055-2016-1-4-3-6.

[5] Blajer, W. and Kołodziejczyk, K.: Dynamics and control of rotary cranes executing a load prescribed motion, Journal of Theoretical and Applied Mechanics, Vol. 44, No. 4, pp. 929-948, 2006.

[6] Carmona, I.G. and Collado, J.: Control of a two wired hammerhead tower crane, Nonlinear Dynamics, Vol. 84, No. 4, pp. 2137-2148, 2016, doi:10.1007/s11071-016-2634-3.

[7] Grigorov, O., Druzhynin, E., Strizhak, V., Strizhak, M., Anishchenko, G.: Numerical simulation of the dynamics of the system "trolley – load – carrying rope" in a cable crane, Eastern-European Journal of

Enterprise Technologies, Vol. 3, No. 7 (93), pp. 6-12, 2018, doi:10.15587/1729-4061.2018.132473.

[8] Kostikov, A.A., Perig, A.V., Mikhieienko, D.Yu., Lozun, R.R.: Numerical JModelica.org-based approach to a simulation of Coriolis effects on guided boom-driven payload swaying during non-uniform rotary crane boom slewing, Journal of the Brazilian Society of Mechanical Sciences and Engineering, Vol. 39, No. 3, pp. 737-756, 2017, doi:10.1007/s40430-016-0554-2.

[9] Kostikov, A.A., Perig, A.V., Lozun, R.R.: Simulation-assisted teaching of graduate students in transport: A case study of the application of acausal freeware JModelica.org to solution of Sakawa's open-loop optimal control problem for payload motion during crane boom rotation, International Journal of Mechanical Engineering Education, Vol. 45, No. 1, pp. 3-27, 2017, doi:10.1177/0306419016669033.

[10] Moon, B.-Y., Hong, S.-R., Ha, M.-T. and Kang, C.-G.: Real-Time Motion Tracking Detection System for a Spherical Pendulum Using a USB Camera, Transactions of the Korean Society of Mechanical Engineers A, Vol. 40, No. 9, pp. 807-813, 2016, doi:10.3795/KSME-A.2016.40.9.807.

[11] Palis, F. and Palis, S.: High performance tracking control of automated slewing cranes, in: Balaguer, C. and Abderrahim, M. (Eds.): *Robotics and Automation in Construction*, InTech, 2008. doi:10.5772/5851.

[12] Perig, A.V., Stadnik, A.N., Deriglazov, A.I.: Spherical Pendulum Small Oscillations for Slewing Crane Motion, The Scientific World Journal, vol. 2014, Article number 451804, 10 pp., 2014, doi:10.1155/2014/451804.

[13] Perig, A.V., Stadnik, A.N., Deriglazov, A.I., Podlesny, S.V.: 3 DOF Spherical Pendulum Oscillations with a Uniform Slewing Pivot Center and a Small Angle Assumption, Shock and Vibration, Vol. 2014, Article number 203709, 32 pp., 2014, doi:10.1155/2014/203709.

[14] Perig, A.V., Stadnik, A.N., Kostikov, A.A., Podlesny, S.V.: Research into 2D Dynamics and Control of Small Oscillations of a Cross-Beam during Transportation by Two Overhead Cranes, Shock and Vibration, Vol. 2017, Article number 9605657, 21 pp., 2017, doi:10.1155/2017/9605657.

[15] Perig, A.V., et al.: Application of JModelica.org to teaching the fundamentals of dynamics of Foucault pendulum-like guided systems to engineering students, Information Technologies and Learning Tools, Vol. 62, No. 6, pp. 151-178, 2017.

[16] Sakawa, Y., Shindo, Y., Hashimoto, Y.: Optimal control of a rotary crane, Journal of Optimization Theory and Applications, Vol. 35, No. 4, pp. 535-557, 1981, doi:10.1007/BF00934931.

[17] Sato, K., Sakawa, Y.: Modelling and control of a flexible rotary crane, International Journal of Control, Vol. 48, No. 5, pp. 2085-2105, 1988, doi:10.1080/00207178808906308.

[18] Sawodny, O., Neupert, J. and Arnold, E.: Actual Trends in Crane Automation – Directions for the Future, FME Transactions, Vol. 37, No. 4, pp. 167-174, 2009.

[19] Li, S. and Jiang, F.: Existence and Stability Analysis on Circular Motion of Pendulums with Uniformly Rotating Pivots, Applied Mathematics and Mechanics, Vol. 39, No. 2, pp. 183-198, 2018, doi:10.21656/1000-0887.380028.

[20] Smoczek, J., Szpytko, J.: Constrained generalized predictive control with particle swarm optimizer for an overhead crane, in: *2017 22nd International Conference on Methods and Models in Automation and Robotics* (*MMAR 2017*), 28-31.08.2017, Miedzyzdroje, Poland, Article number 8046923, pp. 756-761, 2017, doi:10.1109/MMAR.2017.8046923.

[21] Terashima, K., Shen, Y. and Yano, K.: Modeling and optimal control of a rotary crane using the straight transfer transformation method, Control Engineering Practice, Vol. 15, No. 9, pp. 1179-1192, 2007, doi:10.1016/j.conengprac.2007.02.008.

[22] Uchiyama, N., Ouyang, H., Sano, S.: Simple rotary crane dynamics modeling and open-loop control for residual load sway suppression by only horizontal boom motion, Mechatronics, Vol. 23, No. 8, pp. 1223-1236, 2013, doi:10.1016/j.mechatronics.2013.09.001.

[23] Åkesson, J., Årzén, K.-E., Gäfvert, M., Bergdahl, T., Tummescheit, H.: Modeling and optimization with Optimica and JModelica.org – Languages and tools for solving large-scale dynamic optimization problems, Computers & Chemical Engineering, Vol. 34, No. 11, pp. 1737-1749, 2010, doi:10.1016/j.compchemeng.2009.11.011.

[24] Benson, D.A., Huntington, G.T., Thorvaldsen, T.P. and Rao, A.V.: Direct Trajectory Optimization and Costate Estimation via an Orthogonal Collocation Method, Journal of Guidance, Control, and Dynamics, Vol. 29, No. 6, pp. 1435-1440, 2006, doi:10.2514/1.20478.

[25] Magnusson, F., Åkesson, J.: Dynamic Optimization in JModelica.org, Processes, Vol. 3, No. 2, pp. 471-496, 2015, doi:10.3390/pr3020471.

[26] Pontryagin, L.S., Boltyanskii, V.G., Gamkrelidze, R.V. and Mishchenko, E.F.: *The Mathematical Theory of Optimal Processes*, John Wiley and Sons, New York, 1962.

ИСТРАЖИВАЊЕ РЕДУКЦИЈЕ ЊИХАЊА КОРИСНОГ ТЕРЕТА МАНИПУЛАЦИЈОМ ДУЖИНЕ КАБЛА ПРИЛИКОМ КРЕТАЊА СТРЕЛЕ КРАНА

А.А. Костиков, А.В. Периг, О.В. Ларичкин, А.Н. Стадник, Е.П. Грибков

Истражује се динамика управљања стрелом крана проучавањем вођеног кретања корисног терета неравномерним ротирањем стрелом погоњеног средишњег чвора и променљивом дужином кабла. Форму-

лисан је проблем оптималног управљања и нумерички је решен са ограниченом вредношћу дозвољеног њихања корисног терета применом JModelica.org са Optimica екстензијом. Решења оптималне брзине код динамичког модела који описује кретање корисног терета од почетног до крајњег положаја су нађена помоћу нелинеарности повезаних са Кориолисовом силом и променом дужине кабла током кретања. Размотрена су два случаја: са и без ограничења вредности за њихање. Утврђено је да ограничење вредности доводи до пребачаја фазне промене дужине. Добијени резултати се могу користити у различитим областима за пренос терета помоћу крана: индустрији, грађевинарству, итд. Резултат управљања омогућава редуковање времена преноса терета, што доводи до веће продуктивности радне снаге. Такође се смањује њихање корисног терета, па тиме и вероватноћа повређивања приликом утовара и истовара. Модел је нелинеаран и узима у обзир Кориолисову силу и друге нелинеарности. Модел је електро-механички; укључује карактеристике електро-мотора торња и витла. Дата је упоредна анализа проблема оптималног управљања са и без рестрикција вредности за њихање терета и дефинисане су разлике између функција управљања за сваки од датих случајева. Оптимално управљање, узимајући у обзир промену дужине кабла, омогућава изналажење решења за практичне задатке код кретања терета на чијем путу се јављају бројне препреке.